Analyst

PAPER

View Article Online
View Journal

Cite this: DOI: 10.1039/c4an01954g

Real-time detection of H_5N_1 influenza virus through hyperbranched rolling circle amplification

Seyed Vahid Hamidi,[a] Hedayatollah Ghourchian*[a,b] and Gholamreza Tavoosidana*[c]

Received 26th October 2014,
Accepted 12th January 2015

DOI: 10.1039/c4an01954g

www.rsc.org/analyst

An isothermal amplification method was developed for the sensitive detection of the H_5N_1 influenza virus. The padlock probe specifically bound to the H_5N_1 target and circularized with T_4 DNA ligase enzyme. Then this circular probe was amplified by hyperbranched rolling circle amplification (HRCA) using Phi29 DNA polymerase. The fluorescence intensity was recorded at different intervals by intercalation of SYBR green molecules into the double-stranded product of the HRCA reaction. At an optimum time of 88 min, a calibration plot with fine linearity was obtained. Using HRCA based on a padlock probe and Phi29 DNA polymerase, high selectivity and sensitivity were achieved. The biosensor response was linear toward H_5N_1 in the concentration range from 10 fM to 0.25 pM, with a detection limit of 9 fM at a signal/noise ratio of 3. By replacing the heat shock with pH shock, not only was the procedure for detection of H_5N_1 influenza simplified, but also the DNA molecules were protected from possible breaking at high temperature.

Introduction

In the early 21st century, the propagation of avian influenza virus (AIV) involved more than 200 million birds, and 50 million birds died in the European Union within 4 years.[1,2] The influenza virus belongs to the orthomyxoviridae family and is classified based on its genome structure into types A, B and C.[1,3,4] Type A is also classified based on the two different surface antigens, hemagglutinin (HA) and neuraminidase (NA). Today, there are 16 known HA subtypes (H1–H16) and 9 known NA subtypes (N1–N9).[5–7] Among them influenza A virus, subtype H_5N_1, also known as bird flu or A(H_5N_1), is a highly contagious virus found in wild aquatic birds, domestic poultry, and other animal species. The genome of this virus remains stable in these birds.[1,8] Although the transition of H_5N_1 to humans occurs rarely, in the event that this happens it causes great fear and panic due to the high fatality rate. For instance, it caused the death of 6 out of 18 people infected in Hong Kong in 1997.[1,9–11]

Diagnostic methods based on DNA amplification have widely changed scientists' views on viral diagnosis.[12–19] In contrast to polymerase chain reaction (PCR)-based DNA diagnostics, which needs special instrumentation to cycle the temperature, RCA is a powerful and simple technique in which amplification occurs in isothermal conditions.[15,20–23] The amplification process in RCA can be performed either by linear RCA (LRCA) or hyperbranched RCA (HRCA). In LRCA, one primer initiates the reaction and produces a long single strand of DNA. However, in HRCA more than one primer starts the reaction and this produces high molecular weight double-stranded DNA that contains multiple copies of circular DNA.[24–29] By using HRCA it is possible to generate more than 10^9 copies of each circle in 90 minutes, which results a complex pattern of DNA strand displacement.[25] It is also possible to follow the RCA in real time, and quantify the amplification for determination of the target concentration. For this, synthesized fluorogenic indicators, such as molecular beacons or SYBR green, could be utilized.[30–36]

Padlock probe (PLP) is a single-strand circular DNA template that was first introduced by Nilsson *et al.* in 1994. It consists of two specific arms that are placed at 3′ and 5′ sites and are connected to each other *via* a target non-complementary sequence and then, by the action of DNA ligase, the PLP is formed in a circular shape. This process allows very efficient recognition of the target molecules.[24,37–39]

In the present study, by using PLP, HRCA and Phi29 DNA polymerase, a simple RCA technique was developed for real-time detection of H_5N_1 at the femto level. Generally, for DNA denaturation heat shock is used, however, this technique can possibly cause breaking in the DNA molecules due to the application of high temperature. This probably decreases the efficiency of the RCA reaction. In the present work, to overcome this defect the heat shock process was replaced with pH

[a]Laboratory of Microanalysis, Institute of Biochemistry and Biophysics, University of Tehran, P.O. Box 131451384, Tehran, Iran. E-mail: hadi@ibb.ut.ac.ir; Fax: +98 21 66404680; Tel: +98 21 66408920
[b]Nanobiomedicine Center of Excellence, Nanoscience and Nanotechnology Research Center, University of Tehran, P.O. Box 131451384, Tehran, Iran
[c]Department of Molecular Medicine, School of Advanced Technologies in Medicine, Tehran University of Medical Sciences, P.O. Box 1417755469, Tehran, Iran. E-mail: g-tavoosi@tums.ac.ir; Fax: +98 21 88991117; Tel: +98 21 88991118

shock for DNA denaturation. In addition, in most published results[14,27–29,35,40–43] BstI DNA polymerase, with an optimum temperature of 63–65 °C, is used for HRCA. However, in the present work this enzyme was replaced with Phi29 DNA polymerase, which works at room temperature, although its optimum temperature is 30–37 °C. Furthermore, unlike BstI DNA polymerase, the enzyme used in this study does not need exonuclease treatment before HRCA reaction and also has a high ability for the amplification of DNA.

Results and discussion

PLP circularization and HRCA amplification

In order to monitor PLP circularization, the ligation products were separated and monitored using agarose gel. In Fig. 1A, lane 1, PLP was loaded in the linear form. Then, at the end of the electrophoresis its position was used as a control to detect the linear PLP (L-PLP) position in the backside of the C-PLP band. It was observed that C-PLP moved faster than L-PLP because of the packed nature of C-PLP and due to the circularizing process.[24,30] Consequently, at the end of the electrophoresis, the C-PLP (Fig. 1A, lane 2) contained more precursor than the L-PLP (Fig. 1A, lane 1).

To monitor the isothermal amplification of the HRCA reaction, two similar HRCA samples were prepared within 100 min and then the HRCA products, with a wide spectrum of molecular weights, were loaded into the gel. As seen in Scheme 1 (step V), RCA products are produced in concatemeric double-strand DNA form. Therefore, these products have such a high molecular weight that some of the RCA products have remained in the gel and some of them, which are lower in molecular weight, have made smears in the backside of the main product bands (Fig. 1B, lanes 2 and 3).

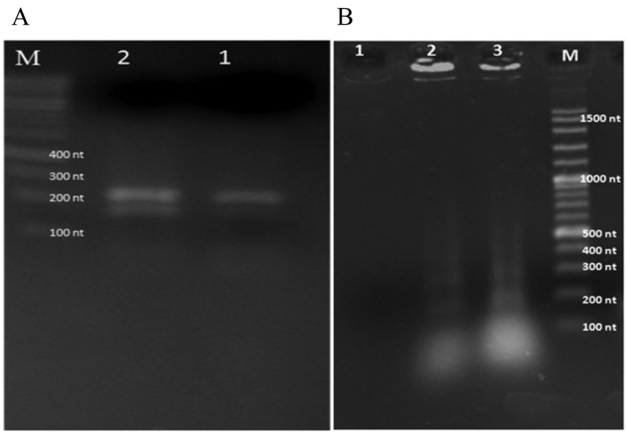

Fig. 1 Gel electrophoresis for identification of PLPs (linear and circular) and HRCA product. (A) Linear and circular forms of PLP made from 112 nucleotide single-strand DNA. Lane M: markers. Lane 1: linear-PLP. Lane 2: circular PLP. (B) Analysis of HRCA product. Lane 1: blank sample (without any target molecule). Lanes 2 and 3: HRCA product. The electrophoresis was carried out using 1% agarose gel (20 cm in length) for 30 min and under the applied voltage of 100 V.

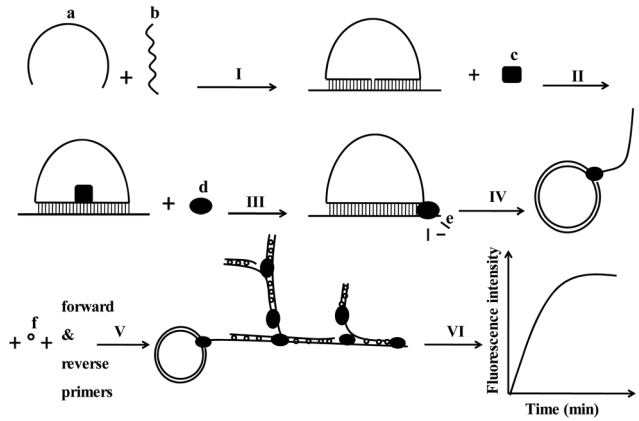

Scheme 1 Representation of the RCA technique for H_5N_1 assay. a: linear PLP (L-PLP), b: H_5N_1 target, c: T_4 DNA ligase enzyme, d: Phi29 DNA polymerase, e: nucleotides, f: SYBR green. I: Combination of the denaturation solution with PLP and H_5N_1 target was followed by the gradual addition of neutralizing solution in order to hybridize PLP with H_5N_1. II: The ligation step for 60 min at 37 °C. During this process DNA ligase seals the adjacent 5′ and 3′ ends of the PLP, thereby creating a circular molecule. III & IV: Phi29 DNA polymerase degrades H_5N_1 from the direction of 3′ to 5′ then uses the 3′ end as a template for initiation of the RCA reaction. V & VI: Circularized probes are amplified by HRCA reaction. This results in a long stretch of concatemer products. As the reaction proceeds, the fluorescence molecules are intercalated in the produced double-strand DNA. This process can be detected by measurement of relative fluorescence intensity in a time course of 100 min at 37 °C.

Optimization of PLP concentration

In order to assay H_5N_1, the effective parameters for quantification of the synthetic target were optimized. At first, the PLP concentration change was studied by recording the fluorescence intensity against time. The HRCA reaction was carried out at 37 °C in the presence of a constant concentration of target but with different concentrations of PLP (Fig. 2). As seen in the inset of Fig. 2, the extra amount of PLP leads to a decrease in the fluorescence signal. To understand the reason for such a decrease in signal, one should imagine that in a concentration ratio of PLP/target of ≤1 there would be high probability for attachment of only one PLP molecule to one target molecule (Reaction 1). But at higher concentrations of PLP (PLP/target >1) there would be the possibility that each PLP molecule could bind to more than one target molecule (Reaction 2). Such a case prevents the circularization process.

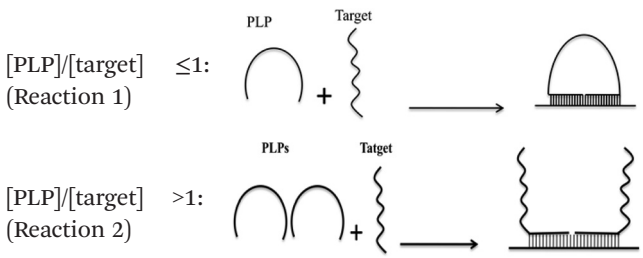

As shown in Fig. 2 (inset), in the presence of a constant concentration of target (0.20 pM), by increasing the PLP concentration up to 0.10 pM the signal reached a plateau then

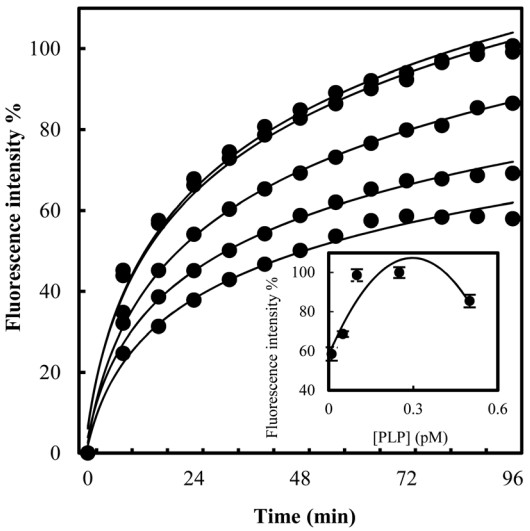

Fig. 2 Optimization of PLP concentration for H_5N_1 assay. The HRCA reaction was carried out at 37 °C in the presence of a constant concentration of target (0.20 pM) and at different concentrations of PLP, from bottom to top: 0.01, 0.05, 0.50, 0.10 and 0.25 pM.

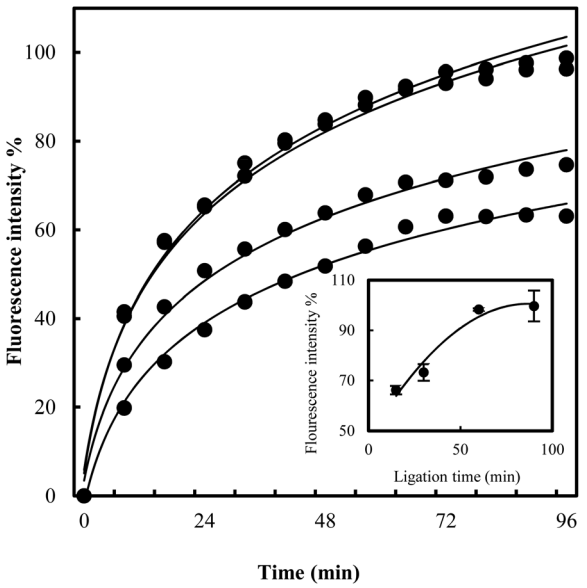

Fig. 3 Fluorescence intensity against time. Ligation reactions were carried out at different times of 15, 30, 60 and 90 min and at 37 °C, in the presence of 0.20 pM H_5N_1 target and 0.12 pM of PLP. Then the fluorescence intensity was recorded *via* real-time RCA. Inset shows the optimum ligation time obtained by comparing the fluorescence intensities at the plateau.

decreased as discussed earlier. A point between 0.10 and 0.25 pM was chosen as the optimized PLP concentration (0.12 pM) throughout this research.

Optimization of ligation time

The optimization of ligation time (the time in which PLP is circularized) was performed at a constant concentration of PLP (0.12 pM) and target (0.20 pM) by following the real-time RCA reaction for 100 min. As shown in Fig. 3, by increasing the ligation time the signal also increased. The maximum signal was achieved after 60 min then it reached a plateau (Fig. 3, inset). Therefore, 60 min was chosen as the optimum ligation time throughout this research.

Enzyme preference

So far different enzymes, such as Phi29 DNA polymerase, Sequenase, Klenow, Vent *exo*-enzymes, and BstI DNA polymerase have been used for the RCA reaction.[20] Among them Phi29 DNA polymerase[20,25,38] and BstI DNA polymerase[20,40,41,44] are the most popular. Although, BstI DNA polymerase has more often been used in the HRCA reaction,[14,27–29,35,40–43] we preferred to use Phi29 DNA polymerase due to its important advantages: (A) it is able to perform the polymerization reaction at moderate temperature (30–37 °C).[30,45,46] (B) It is highly processive, so that the amplification reaction continues up to 70 000 nucleotides while it is still joined to the DNA template. The synthesis rate was reported to be ~1500 nucleotides per min.[45,47,48] This, of course, could improve the sensitivity of the assay. (C) Phi29 DNA polymerase degrades the target from 3′ to 5′ then it uses the 3′ as a primer for the RCA reaction, called target-primed RCA.[49,50] So, in contrast to BstI DNA polymerase, Phi29 DNA polymerase doesn't require the use of an exonuclease enzyme prior to the amplification reaction.

Calibration curve for H_5N_1

In view of the fact that influenza viruses are variant, it was important to evaluate the performance of the biosensor in the presence of real H_5N_1 samples that may contain possible single nucleotide polymorphisms. Therefore, in order to prepare the calibration curve, seven different real H_5N_1 samples from birds, were obtained from the Tehran University of Medical Science and tested in compliance with the relevant laws and institutional guidelines and their concentrations were determined by conventional real-time PCR (Fig. 4A). Also, the relevant experimental procedure was approved by the animal care committee of Tehran University of Medical Science. Thereafter, the RCA signals for the standard real H_5N_1 samples were recorded against time. As seen, by increasing the concentration of target, the signal intensity increased drastically over time and finally reached a plateau (Fig. 4A). Since the signal at 88 min was more reproducible and linear (Fig. 4B), this time was selected as the fluorescence signal end point value.

Finally, the calibration curve for the real H_5N_1 targets was plotted by recording the RCA signal at different concentrations of target at 88 min. As seen, using this procedure H_5N_1 was monitored in the concentration range from 10 fM to 0.25 pM (Fig. 4B). The detection limit (DL) at a signal to noise ratio of 3 (S/N = 3) was calculated according to eqn (1):

$$\mathrm{DL} = 3.3\sigma/S \quad (1)$$

where σ is standard deviation of the response and S is the slope of the curve.[51]

The regression equation for the H_5N_1 calibration curve was: $I = 252.8[H_5N_1] - 36.59$ ($R = 0.993$, $n = 3$), and the relative stan-

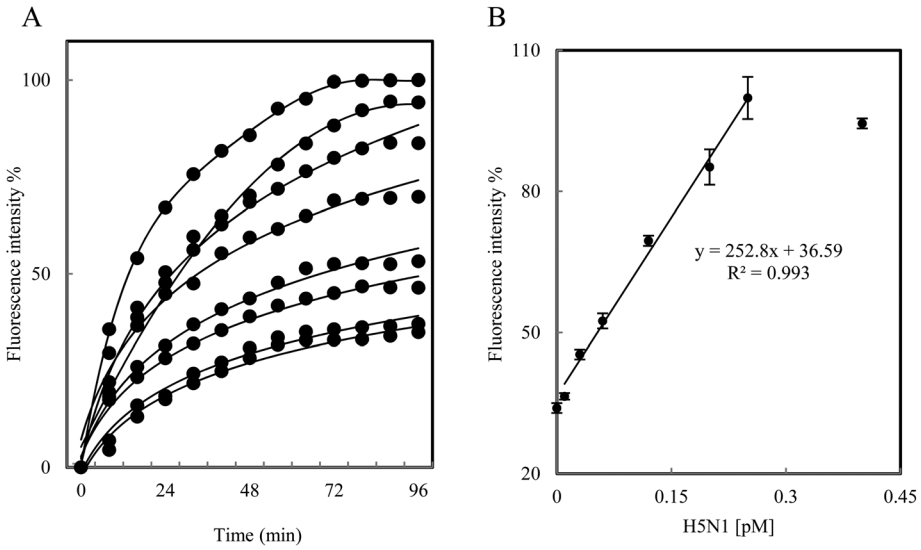

Fig. 4 (A) Fluorescence intensity against time at different concentrations of real H_5N_1 samples. The real-time RCA signal was recorded at different H_5N_1 real sample concentrations, from bottom to top: 0, 0.01, 0.03, 0.06, 0.12, 0.20, 0.40 and 0.25 pM at 37 °C. (B) The calibration curve for the real H_5N_1 samples.

dard deviation of the biosensor response at a concentration of 0.03 pM was 0.70% for three successive measurements. Based on eqn (1), the detection limit was calculated to be as low as 9 fM, at a signal/noise ratio of 3.

As seen in Fig. 4A, at zero concentration of H_5N_1, a background of about 30% fluorescence intensity was observed. To understand the source of this background it is worth noting that in the absence of H_5N_1 the PLP could not be circularized, however, it can be hybridized with the forward primer (to recognize this sequence compare the PLP and forward primer sequences in Table 1) and form a double-stranded oligonucleotide with 47 base pairs at most. Consequently, SYBR green is intercalated in the oligonucleotide and produces a limited signal as background. It is worth noting that in order to check the repeatability of the biosensor responses, each measurement was repeated three times and the results were reported as error bars in the figures.

As compared in Table 2, the analytical parameters, such as detection limit and linear range, obtained by the present method were much improved relative to those parameters reported in the literature.[30,52–55] The reason for such improvements could be attributed to the nature of the amplifying process in HRCA. Using this process it is possible to generate more than 10^9 copies of each circle, which results in a huge signal amplification *via* DNA ramification.[25] The possibility for following the RCA in real time, and the usage of a sensitive fluorescence plate reader device as the detector are two other advantages that provide better sensitivity and an improved detection limit for H_5N_1 assay. The application of PLP is another advantage of this system that led to the recognition of the target molecules very efficiently *via* completion of the hybridization of the 3′ and 5′ ends of the PLP to the target and ligation of the circular probe from head to tail,[56,57] as shown in Scheme 1. More improvement in this system was obtained by the use of pH shock instead of heat shock. This not only makes the method simpler but also preserves the DNA structure from potential breaking. In addition, it enables the whole procedure to be carried out at low isothermal temperature. This is the reason we were able to improve the detection limit down to the fM level. It is also important to note that this biosensor is label-free, which makes it much more simple. Consequently, on the one hand the replacement of heat shock by pH shock simplifies the system and improves its sensitivity and on the other hand escaping from the labeling process makes the method easy to setup. It seems that these advantages help the system to be more applicable for commercial purposes.

Table 1 The sequences for the PLP, primers and target[a,b]

Type of oligonucleotides	Sequence
PLP[1]	5′ P-GGATGATCTGAATTTTCTCAAACCCGGTCAACTTCAAGCTCCTAAGCCTTGACGAA CCGCTTTGCCTGACTGAATGCAGCGTAGGTATCGACTTCGGACCAAGAACTTTTGG-3′
Forward primer	5′-GCTTAGGAGCTTGAAGTTG*A*C-3′
Reverse primer	5′-GCTTTGCCTGACTGAATGC*A*G-3′
H_5N_1 target	5′-TTTGAGAAAATTCAGATCATCCCCAAAAGTTCTTGGTCCGA-3′

[a] P at the 5′-end of the probe indicates phosphorylation. [b] The stars (*) at the 3′-end of the primers indicate phosphorothioate modifications.

Table 2 Comparison of analytical parameters obtained by the RCA method for different targets

Target	Detection method	Linear range (pM)	Detection limit (pM)	References
H_5N_1 gene	Fluorescence	0.01–0.25	0.009	Present work
β-Thalassemia gene	Ultraviolet (UV)	0.30–80	0.07	52
PDGF	Fluorescence	300–80 000	300	30
Streptavidin	Electrochemical	1–500 000	0.4	53
Epididymis-specific protein 4	Electrochemical	3–300	0.06	54
PDGF	Electrochemical	84–8400	63	55

Specificity

Specificity is an important factor in analyzing a complex biological matrix. In this study, the specificity of the method was determined by comparing the signal obtained for H_5N_1 as the target with those for hepatitis B virus (HBV), genomic DNA, H_7N_7 and H_3N_8 as unspecific targets. A significant signal was observed for H_5N_1, while the signals for blank (negative control), HBV, genomic DNA, and two subtypes of influenza A virus that have been found in birds including H_7N_7 and H_3N_8 were the same as that of the background (Fig. 5). In view of the fact that the target was designed based on the most specific and conserved part of the H_5N_1 HA gene and due to accurate hybridization and circularization, PLP was able to detect the H_5N_1 virus very specifically (Fig. 5).

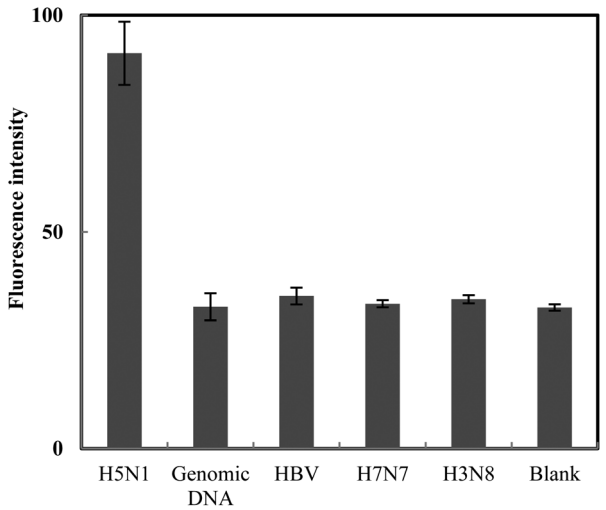

Fig. 5 Comparison of the specificity of the HRCA biosensor towards different DNA samples. The real-time HRCA signal was recorded toward different synthetic molecules of H_5N_1, genomic DNA, HBV, H_7N_7, H_3N_8 and blank as a negative control. All samples were used at 0.25 pM concentration. The experiments were carried out at 37 °C and at a PLP concentration of 0.12 pM.

In addition, in order to prove the selectivity of PLP toward H_5N_1, both specific arms of PLP were aligned with segment 4 of the H_3N_8 and H_7N_7 genomes (which encode the HA gene in all subtypes of the influenza A virus) by utilizing basic local alignment search tool (BLAST) software (http://blast.ncbi.nlm.nih.gov/Blast.cgi). The maximum score obtained for the alignment of the specific arms with the HA genes of H_3N_8 and H_7N_7, was 16.4, which is too low for it to be specifically detected. Therefore, the PLP cannot be circularized to be used as a template in the RCA reaction. It is also noticeable that influenza A viruses exchange their genomic segments *via* the mechanism of antigenic shift, which occurs when two different influenza A strains combine and infect the same cell. Therefore, it is possible for the genomic segments to be transferred from one strain to another one. According to the sequences provided by the genomic database (www.ncbi.nlm.nih.gov), the recognition region for the proposed PLP also exists in the H_5N_5 subtype. However, the frequency of the reported target is too low (one out of 100, sequence ID: gb|JX878683.1). Thus, the veracity of this report is doubtful.

Feasibility for real samples

In order to investigate the feasibility of the proposed biosensor for the determination of H_5N_1 in real samples, seven specimens obtained from sick birds were examined. First, the concentrations of H_5N_1 in the real positive samples were determined to be 0.18, 0.14, 0.14, 0.19, 0.18, 0.14 and 0.18 pM using standard real-time PCR. Then, the fluorescence intensities of these samples were recorded by the proposed biosensor. Based on the calibration curve reported in Fig. 4B, the concentrations of H_5N_1 in the real positive samples were determined to be 0.16 ± 0.002, 0.13 ± 0.004, 0.12 ± 0.006, 0.17 ± 0.003, 0.15 ± 0.004, 0.13 ± 0.005 and 0.17 ± 0.004 pM (Table 3). As seen, there is a satisfactory consistency between the data obtained by standard real-time PCR and the RCA-based biosensor. This indicates the feasibility of the proposed biosensor for the determination of H_5N_1 in clinical analysis.

Table 3 The biosensor responses for determination of H_5N_1 in real bird serum samples. Before measurement with the RCA-based biosensor, control measurements were taken on these samples using the conventional real-time PCR technique

Methods	Sample 1 (pM)	Sample 2 (pM)	Sample 3 (pM)	Sample 4 (pM)	Sample 5 (pM)	Sample 6 (pM)	Sample 7 (pM)
Present biosensor	0.16 ± 0.002	0.13 ± 0.004	0.12 ± 0.006	0.17 ± 0.003	0.15 ± 0.004	0.13 ± 0.005	0.17 ± 0.004
Real-time PCR	0.18	0.14	0.14	0.19	0.18	0.14	0.18

Experimental

Chemicals

The length of PLP used in this assay was 112 nucleotides. This circularizable oligonucleotide probe consisted of two adjacent complementary sequences, which were chosen from the most conserved parts of the H_5N_1 HA gene by utilizing the BioEdit Sequence Alignment Editor software (19 and 22 nt). Also, it has a linker region (71 nt) to facilitate the formation of the circular template and provide spaces for RCA primer binding. Since the target sequence is identical for this subtype, it can only detect the H_5N_1 subtype of the influenza A virus.[1,58,59] Furthermore, the conservation of the PLP binding site was evaluated by utilizing BLAST for analysis of the sequence. After performing BLAST, the recognition site for PLP was 100 percent identical in all HA genes of the H_5N_1 virus that were reported in the genomic database. This means that this PLP has the capability to detect all variants of the H_5N_1 virus.

The 5′ phosphorylated linear PLP and oligonucleotides (synthetic target and 3′ phosphorothioate modified primers) were purchased from Metabion (Martinsried, Germany). The primers, probe and synthetic target are listed in Table 1. The RevertAid First Strand cDNA Synthesis Kit, T_4 ligase buffer, T_4 ligase enzyme, Phi29 buffer, Phi29 DNA polymerase, deoxyribonucleotide triphosphate (dNTP) and SYBR green I were obtained from Fermentas (USA). KOH and HCl were purchased from Merck (Germany). Ethylenediaminetetraacetic acid (EDTA), Tris-HCl, agarose, Tris-acetate and ethidium bromide were purchased from Sigma-Aldrich (USA). The RNA extraction kit, real-time PCR kit and 384 well plates were respectively obtained from Jena Bioscience (Germany), Genesig (United Kingdom) and Greiner Bio-One (Germany). In all experiments the solutions were prepared by using double-distilled deionized water. And all chemicals were used without further purification.

Apparatus

Virus cDNA was synthesized in an Eppendorf thermocycler (Germany). Electrophoresis was performed in an Akhtarian electrophoresis tank (Tehran, Iran) and the voltage was adjusted with a Bio-rad power supply (California, USA). The gel was visualized with a SynGen transilluminator (United Kingdom). The fluorescence emissions were recorded at 520 nm with a fluorescence microplate reader (H4, Bio Tech Co, USA). Real-time PCR was carried out using a Rotor-Gene Qiagen real-time PCR cycler (USA).

Virus samples and cDNA synthesis. The infected samples were obtained from sick birds. RNA was extracted using an RNA extraction kit and cDNA was synthesized with a RevertAid First Strand cDNA Synthesis Kit, in which the temperature was adjusted in a thermocycler.

PLP ligation and hyperbranched rolling circle amplification. 1 μl of cDNA from the H_5N_1 virus, 1 μl of PLP and 1.2 μl of denaturing solution (pH 12) containing 400 mM KOH and 10 mM EDTA were mixed (by pipetting the mixture up and down) and incubated for 3 min at room temperature. Then, 0.8 μl of neutralizing buffer containing 600 mM Tris-HCl and 400 mM HCl was injected in to the reaction mixture gradually (if this process is carried out precisely, the exact final pH will be 7.9). Afterward, 6 μl of the ligation mixture containing 1 μl of 10× T_4 ligase buffer (consisting of 400 mM Tris-HCl, 100 mM $MgCl_2$, 100 mM DTT, and 5 mM ATP, at pH 7.9) and 5 μl deionized water were added to the reaction mixture. The ligation reaction was carried out by the addition of 2 units (U) of T_4 ligase to the mixture and incubating at 37 °C for 60 min. The ligation reactions were terminated by heating at 70 °C for 5 min. Thereafter, 40 μl of the RCA mixture containing a final concentration of 1× Phi29 buffer (33 mM Tris-acetate (pH 7.9), 10 mM Mg-acetate, 66 mM K-acetate, 1% (v/v) Tween 20, 1 mM DTT), 500 μM dNTP, 10 pM forward primer, 10 pM reverse primer, 8 U of Phi29 DNA polymerase and 1× SYBR green I was added to 10 μl ligation reaction mixtures. The mixture (50 μl) was poured into a well. The plate was placed in a fluorescence plate reader device and the real-time fluorescence intensity was recorded for 100 min at 37 °C. To stop the reactions the mixture was incubated at 65 °C for 10 min and finally stored at 4 °C. Therefore, the total time taken to run the RCA technique for H_5N_1 assay (Scheme 1) was about 180 min.

Gel electrophoresis assay. Electrophoretic analysis of PLP, C-PLP (circular padlock probe) and HRCA products was performed in 1% agarose gels filled with TAE buffer (40 mM Tris-acetate, 1 mM EDTA, pH 8.0). This process was carried out for 30 min under an applied voltage of 100 V. Then the gel was stained by ethidium bromide and visualized with a trans-illuminator at 302 nm.[24]

Real sample detection. The designed RCA technique was evaluated by quantification of seven real samples. The results were compared with those obtained by the standard method of real-time PCR using a real-time PCR kit. It is important to note that the H_5N_1 specific primers that were amplified by PCR contained about 130 bases within the conserved portion of the H_5N_1 HA gene.

Conclusion

The detection limit (9 fM) and linear range (10 fM to 0.25 pM) obtained by the present isothermal amplification technique brings us to the conclusion that the integrating of PLP, HRCA, Phi29 DNA polymerase and the pH shock process has much improved the sensitivity, specificity and linearity of the RCA-based biosensor toward the H_5N_1 virus, relative to those methods reported in the literature. Compared to the conventional PCR technique, the method shows some advantages such as isothermal amplification and higher sensitivity. Also, comparison between the data obtained by standard real-time PCR and the RCA-based biosensor proved the reliability of the method. In addition, by applying Phi29 DNA polymerase and the pH shock process, the HRCA reaction could be performed at moderate temperature. Therefore, it seems that the proposed biosensor has the potential to be used as a user friendly

DNA diagnostic method for the determination of H_5N_1 in clinical analysis.

Acknowledgements

The financial support provided by the Research Council of the University of Tehran and the Tehran University of Medical Sciences is acknowledged.

References

1 P. Gyarmati, T. Conze, S. Zohari, N. LeBlanc, M. Nilsson, U. Landegren, J. Banér and S. Belák, *J. Clin. Microbiol.*, 2008, **46**, 1747–1751.
2 I. Capua and S. Marangon, *Emerg. Infect. Dis.*, 2006, **12**, 1319.
3 K. V. Reeth, *Vet. Res.*, 2007, **38**, 243–260.
4 R. G. Webster, W. J. Bean, O. T. Gorman, T. M. Chambers and Y. Kawaoka, *Microbiol. Rev.*, 1992, **56**, 152–179.
5 S. Payungporn, S. Chutinimitkul, A. Chaisingh, S. Damrongwantanapokin, C. Buranathai, A. Amonsin, A. Theamboonlers and Y. Poovorawan, *J. Virol. Methods*, 2006, **131**, 143–147.
6 R. A. M. Fouchier, V. Munster, A. Wallensten, T. M. Bestebroer, S. Herfst, D. Smith, G. F. Rimmelzwaan, B. Olsen and A. D. M. E. Osterhaus, *J. Virol.*, 2005, **79**, 2814–2822.
7 A. P. Nguyen and K. M. Downard, *Analyst*, 2013, **138**, 1787–1793.
8 K. M. Sturm-Ramirez, T. Ellis, B. Bousfield, L. Bissett, K. Dyrting, J. E. Rehg, L. Poon, Y. Guan, M. Peiris and R. G. Webster, *J. Virol.*, 2004, **78**, 4892–4901.
9 E. C. J. Claas, A. D. M. E. Osterhaus, R. van Beek, J. C. De Jong, G. F. Rimmelzwaan, D. A. Senne, S. Krauss, K. F. Shortridge and R. G. Webster, *Lancet*, 1998, **351**, 472–477.
10 K. Subbarao, A. Klimov, J. Katz, H. Regnery, W. Lim, H. Hall, M. Perdue, D. Swayne, C. Bender, J. Huang, M. Hemphill, T. Rowe, M. Shaw, X. Xu, K. Fukuda and N. Cox, *Science*, 1998, **279**, 393–396.
11 J. Peiris, W. Yu, C. Leung, C. Cheung, W. Ng, J. M. Nicholls, T. Ng, K. Chan, S. Lai, W. Lim, K. Y. Yuen and Y. Guan, *Lancet*, 2004, **363**, 617–619.
12 V. V. Demidov, *Expert Rev. Mol. Diagn.*, 2003, **3**, 121–124.
13 H. Shikata, N. Utsumi, H. Kuivaniemi and G. Tromp, *J. Lab. Clin. Med.*, 1995, **125**, 421–432.
14 I. V. Smolina, V. V. Demidov, C. R. Cantor and N. E. Broude, *Anal. Biochem.*, 2004, **335**, 326–329.
15 M. M. Ali, F. Li, Z. Zhang, K. Zhang, D. K. Kang, J. A. Ankrum, X. C. Le and W. Zhao, *Chem. Soc. Rev.*, 2014, **43**, 3324–3341.
16 A. Niemz, T. M. Ferguson and D. S. Boyle, *Trends Biotechnol.*, 2011, **29**, 240–250.
17 W. Zhao, M. M. Ali, M. A. Brook and Y. Li, *Angew. Chem., Int. Ed.*, 2008, **47**, 6330–6337.
18 I. Weibrecht, K. J. Leuchowius, C. M. Clausson, T. Conze, M. Jarvius, W. M. Howell, M. Kamali-Moghaddam and O. Söderberg, *Expert Rev. Proteomics*, 2010, **7**, 401–409.
19 D. Haible, S. Kober and H. Jeske, *J. Virol. Methods*, 2006, **135**, 9–16.
20 V. V. Demidov, *Expert Rev. Mol. Diagn.*, 2002, **2**, 542–548.
21 A. Rector, R. Tachezy and M. Van Ranst, *J. Virol.*, 2004, **78**, 4993–4998.
22 A. Zieba, K. Grannas, O. Söderberg, M. Gullberg, M. Nilsson and U. Landegren, *New Bioeth.*, 2012, **29**, 634–640.
23 M. Stougaard, S. Juul, F. F. Andersen and B. R. Knudsen, *Integr. Biol.*, 2011, **3**, 982–992.
24 H. Kuhn, V. V. Demidov and M. D. Frank-Kamenetskii, *Nucleic Acids Res.*, 2002, **30**, 574–580.
25 P. M. Lizardi, X. Huang, Z. Zhu, P. Bray-Ward, D. C. Thomas and D. C. Ward, *Nat. Genet.*, 1998, **19**, 225–232.
26 D. Yong Zhang, M. Brandwein, T. Chun Hung Hsuih and H. Li, *Gene*, 1998, **211**, 277–285.
27 D. C. Thomas, G. A. Nardone and S. K. Randall, *Arch. Pathol. Lab. Med.*, 1999, **123**, 1170–1176.
28 G. Hafner, I. Yang, L. Wolter, M. Stafford and P. Giffard, *BioTechniques*, 2001, **30**, 852–867.
29 D. Y. Zhang, W. Zhang, X. Li and Y. Konomi, *Gene*, 2001, **274**, 209–216.
30 L. Yang, C. W. Fung, E. J. Cho and A. D. Ellington, *Anal. Chem.*, 2007, **79**, 3320–3329.
31 D. A. Di Giusto, W. A. Wlassoff, J. J. Gooding, B. A. Messerle and G. C. King, *Nucleic Acids Res.*, 2005, **33**, e64.
32 M. Nilsson, M. Gullberg, F. Dahl, K. Szuhai and A. K. Raap, *Nucleic Acids Res.*, 2002, **30**, e66.
33 J. J. Harvey, S. P. Lee, E. K. Chan, J. H. Kim, E. S. Hwang, C. Y. Cha, J. R. Knutson and M. K. Han, *Anal. Biochem.*, 2004, **333**, 246–255.
34 I. V. Smolina, V. V. Demidov, V. A. Soldatenkov, S. G. Chasovskikh and M. D. Frank-Kamenetskii, *Nucleic Acids Res.*, 2005, **33**, e146.
35 J. Yi, W. Zhang and D. Y. Zhang, *Nucleic Acids Res.*, 2006, **34**, e81.
36 H. Zhou, K. Bouwman, M. Schotanus, C. Verweij, J. Marrero, D. Dillon, J. Costa, P. Lizardi and B. Haab, *Genome Biol.*, 2004, **5**, R28.
37 M. Nilsson, H. Malmgren, M. Samiotaki, M. Kwiatkowski, B. Chowdhary and U. Landegren, *Science*, 1994, **265**, 2085–2088.
38 J. Banér, M. Nilsson, M. Mendel-Hartvig and U. Landegren, *Nucleic Acids Res.*, 1998, **26**, 5073–5078.
39 Y. Wang, M. Cottman and J. D. Schiffman, *Cancer Genet.*, 2012, **205**, 341–355.
40 S. Kaocharoen, B. Wang, K. M. Tsui, L. Trilles, F. Kong and W. Meyer, *Electrophoresis*, 2008, **29**, 3183–3191.
41 J. Y. Marciniak, A. C. Kummel, S. C. Esener, M. J. Heller and B. T. Messmer, *BioTechniques*, 2008, **45**, 275.

42 Y. Long, X. Zhou and D. Xing, *Biosens. Bioelectron.*, 2011, **26**, 2897–2904.
43 A. Cao and C. Y. Zhang, *Anal. Chem.*, 2012, **84**, 6199–6205.
44 M. C. Steain, D. E. Dwyer, A. C. Hurt, C. Kol, N. K. Saksena, A. L. Cunningham and B. Wang, *Antiviral Res.*, 2009, **84**, 242–248.
45 R. Johne, H. Müller, A. Rector, M. Van Ranst and H. Stevens, *Trends Microbiol.*, 2009, **17**, 205–211.
46 J. R. Nelson, Y. C. Cai, T. L. Giesler, J. W. Farchaus, S. T. Sundaram, M. Ortiz-Rivera, L. P. Hosta, P. L. Hewitt, J. A. Mamone and C. Palaniappan, *BioTechniques*, 2002, **32**, 44–47.
47 S. Margeridon, S. Carrouée-Durantel, I. Chemin, L. Barraud, F. Zoulim, C. Trépo and A. Kay, *Antimicrob. Agents Chemother.*, 2008, **52**, 3068–3073.
48 L. Blanco, A. Bernad, J. M. Lázaro, G. Martín, C. Garmendia and M. Salas, *J. Biol. Chem.*, 1989, **264**, 8935–8940.
49 C. Larsson, J. Koch, A. Nygren, G. Janssen, A. K. Raap, U. Landegren and M. Nilsson, *Nat. Methods*, 2004, **1**, 227–232.
50 H. L. Wamsley and A. F. Barbet, *J. Clin. Microbiol.*, 2008, **46**, 2314–2319.
51 K. Du, Y. Zhou, L. Wang and Y. Wang, *J. Appl. Polym. Sci.*, 2009, **113**, 1966–1974.
52 J. Li, T. Deng, X. Chu, R. Yang, J. Jiang, G. Shen and R. Yu, *Anal. Chem.*, 2010, **82**, 2811–2816.
53 Q. Wang, B. Jiang, J. Xie, Y. Xiang, R. Yuan and Y. Chai, *Analyst*, 2013, **138**, 5751–5756.
54 L. Lu, B. Liu, Z. Zhao, C. Ma, P. Luo, C. Liu and G. Xie, *Biosens. Bioelectron.*, 2012, **33**, 216–221.
55 Z. S. Wu, H. Zhou, S. Zhang, G. Shen and R. Yu, *Anal. Chem.*, 2010, **82**, 2282–2289.
56 M. Nilsson, *Histochem. Cell Biol.*, 2006, **126**, 159–164.
57 U. Landegren, R. Kaiser, J. Sanders and L. Hood, *Science*, 1988, **241**, 1077–1080.
58 B. Wang, S. J. Potter, Y. Lin, A. L. Cunningham, D. E. Dwyer, Y. Su, X. Ma, Y. Hou and N. K. Saksena, *J. Clin. Microbiol.*, 2005, **43**, 2339–2344.
59 T. Hall, *GERF Bull. Biosci.*, 2011, **2**, 60–61.